Hybrid FEA and Meta-modeling for DE Optimization of a Highly Saturated Spoke IPM

Oluwaseun A. Badewa[1], Marcelo D. Silva[2], Rosemary E. Alden[1], Pedram Asef[3], and Dan M. Ionel[1]

[1]SPARK Laboratory, Stanley and Karen Pigman College of Engineering, University of Kentucky, Lexington, KY, USA
[2]Department of Electrical Engineering, Uppsala University, Uppsala, Sweden
[3]Advanced Propulsion Laboratory (APL), Department of Mechanical Engineering, University College London, London, UK
o.badewa@uky.edu, marcelo.silva@angstrom.uu.se, rosemary.alden@uky.edu, pedram.asef@ucl.ac.uk, dan.ionel@ieee.org

***Abstract*—This paper introduces a novel approach for high-performance electric motor design that combines machine learning (ML)-based meta-modeling with a differential evolution (DE) optimization algorithm. The method leverages finite element analysis (FEA) results to train the ML meta-model, enabling efficient design optimization for high-power density cored machines, such as spoke interior permanent magnet motors (IPM), which exhibit complex nonlinearities and saturation effects. This hybrid ML-DE framework seeks to provide an alternative for physics-based electric motor design and optimization, offering significant reductions in computational effort while maintaining accuracy. The meta-model's accuracy in capturing the nonlinear relationships between design parameters, core losses, and torque is assessed using metrics such as R-squared (R^2), normalized root mean square error (NRMSE), and mean absolute percentage error (MAPE), showing promising performance.**

***Index Terms*—Meta-modeling, machine learning, artificial intelligence, differential evolution, finite element analysis, synchronous motor, spoke-type PM, interior PM motor.**

I. Introduction

With the increasing deployment of electric motors in various applications, including traction and propulsion, the need for tailored high motor performance has become essential [1]–[4]. Consequently, selecting a motor topology and optimizing its design is crucial, especially in light of conflicting objectives such as cost, efficiency, weight, and power density [3], [5], [6]. Amongst the several motor topologies adopted for electric mobility, such as the induction motor (IM) [7], [8], synchronous reluctance motor (SynRM) [9], [10], interior permanent magnet motor (IPM) [11]–[13], and axial flux permanent magnet (AFPM) motor [14], [15], the spoke-type PM motors have emerged as a promising candidate. Belonging to the general class of synchronous motors, these motors exhibit high power density due to flux intensification, along with benefits such as low torque ripple, reduced losses, and modular construction [16]–[20].

Furthermore, the design optimization of electrical machines presents a nonlinear multi-objective challenge, requiring a balance between competing goals such as maximizing efficiency, minimizing cost, and reducing the weight of active materials. Beyond electromagnetic performance, this process must also account for mechanical, thermal, and material constraints [5], [21]. Several deterministic and stochastic approaches that have been adopted to solve this nonlinear problem include the sequential unconstrained minimization technique (SUMT), the Genetic Algorithm (GA), Simulated Annealing, Particle Swarm Optimization (PSO), and Differential Evolution (DE). Multi-objective differential evolution (MODE) inspired by the natural evolution process, has become widely used for motor design [5], [22].

Recently, to take advantage of the advancements in big data and large-scale computation, strategies employing artificial intelligence (AI), machine learning (ML), and deep learning (DL) have been proposed for motor design and optimization [23]–[26]. The development of meta-models, also known as surrogate models, based on these large data has, therefore, been the focus of numerous exploratory studies [27]. Typically, the meta-models in these studies are based on various Neural Networks (NN) architectures, such as Artificial Neural Networks (ANNs) [28], Convolutional Neural Networks (CNNs) [29], and Generative Adversarial Network (GAN) solutions [30]. Many of these meta-models are designed for use in optimization contexts, where they serve to reduce the number of Finite Element Method (FEM)- based simulations through their integration with optimization processes using evolutionary algorithms [27], [31]–[33].

This paper explores the feasibility of using an ANN meta-model, trained with minimal FEA data obtained through DE, to predict performance metrics of highly saturated, nonlinear spoke-type IPM designs. The approach aims to emulate FEA, enabling faster design optimization and increased flexibility. This is distinct from typical methods of ANN training using dedicated sampling techniques, such as Latin hypercube sampling or the Sobol sequence, and seeks to provide benefits of reduced computational effort for design optimization, precise predictions with suitable training, and scalable output torque per stack length for higher-torque-output designs. The motor topology is reviewed in the subsequent sections, followed by the design optimization, which includes the proposed new method. The results obtained are then discussed, followed by a conclusion.

II. Motor Topology and Design

The example machine shown in Fig. 1, and employed as a reference in the current study, is a prototype IPM motor,

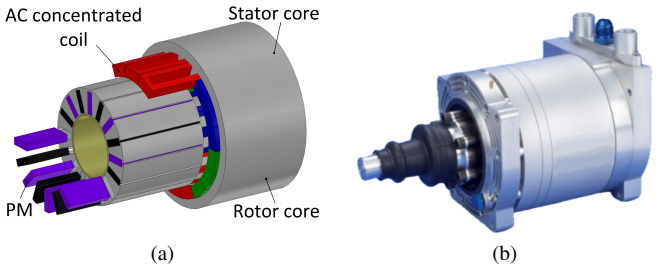

(a) (b)

Fig. 1. The studied spoke IPM machine showing (a) an exploded view of a solid model with concentrated AC coils and spoke-type PMs and (b) a prototype motor designed for electric racing.

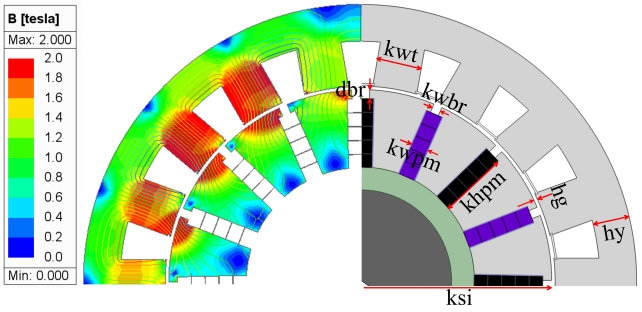

Fig. 2. Cross-sectional view of spoke IPM design showing flux lines, high saturation, and 8 labeled geometric independent variables considered in the multi-objective optimization.

which was originally designed as part of the developments for the first generation formula E [34]. The machine has been further optimized, prototyped, and tested as described in more detail in [16], [17]. This design has a very high airgap flux density, high magnetic saturation in the core, and demonstrated at the time, ultra high power density. The IPM motor employs a spoke rotor with 16 poles and very high flux concentration and uses high-energy PMs. The stator has a 3-phase winding with concentrated coils and special laminated electric steel.

The airgap flux density, B_{ag}, for this spoke-type PM motor can be obtained as:

$$B_{ag} = B_r \left(\frac{\pi D_g}{4 k_\sigma p h_{PM}} + \frac{2 \mu_r g}{w_{PM}} \right)^{-1}, \tag{1}$$

where, D_g is the airgap diameter, p the number of pole pairs, g the airgap height, μ_r the PM relative permeability, B_r the PM remanent flux density, and k_σ the leakage coefficient, which can be adjusted to account for the saturation and slotting effect, w_{PM} the PM length in the direction of magnetization, and h_{PM} the PM height along the radius. The electromagnetic torque, T_e, can also be obtained as:

$$T_e = \frac{3}{2} p \left[\lambda_{pm} i_q + (L_d - L_q) i_d i_q \right] \tag{2}$$

where λ_{pm} is the permanent magnet flux linkage, i_d and i_q are the stator currents in the d- and q-axes, respectively, and L_d and L_q are the inductances in the d- and q-axes, respectively. The spoke-type rotor in this machine has the great benefit of flux concentration. It also provides mechanical retention of the magnet blocks, making it suitable for high-speed and high-performance applications such as racing cars or industrial drives, where direct-drive solutions are favored for both motor and regenerative braking operations [35].

The performance of this motor topology is greatly influenced by the quality of materials used. For power density and reliability, high-energy PM materials such as neodymium iron boron (NdFeB) and samarium cobalt (SmCo) are commonly selected, depending on the application's thermal management and cost constraints. Sintered SmCo has been selected due to its ability to withstand elevated temperatures without significant loss of magnetization. For the ferrous core, non-oriented silicon-iron steel with a thin lamination gauge has been employed to limit eddy currents and manage the effects of high-frequency harmonics [16].

Amongst the available choices for slot-pole combination, the 18-slot/16-pole configuration was considered to be optimal for achieving a high winding factor, minimizing undesirable harmonics, and minimizing the unbalanced magnetic pull. The fractional-slot concentrated windings provide a high fundamental winding factor, ensuring efficient MMF distribution and reducing the impact of higher-order harmonics that could lead to increased losses in the core and windings [36]. This configuration has, therefore, been selected for design optimization and analyses in the subsequent sections.

III. DE and FEA for ML Training

A. Sensitivity analysis

Considering a fixed stator outer diameter of 160mm and base speed of 6,000rpm, the developed 18s16p 2D FEA model for analyses is shown in Fig. 2 with 8 independent geometric variables as detailed in Table I [37]. These geometric variables control key features of this motor topology, which directly influence its performance. To study the relationship between these geometric variables and motor performance at peak electrical loading, a sensitivity analysis employing a design of experiments (DoE) has been used. A central composite design (CCD) approach was utilized to generate the necessary FEA parametric models. These models were analyzed and then fitted with a regression curve to establish a relationship between the independent variables and performance metrics [5], [19], [38].

For performance indexes of active mass, motor loss, and torque, their sensitivity to the independent geometric variables is summarized in Fig. 3. In line with expectations in this highly saturated machine, the airgap length, stator yoke thickness, and PM thickness in the direction of magnetization influence torque the most. Variables responsible for the thickness of the stator teeth, yoke, and rotor core are closely tied to the active mass. The split ratio is most influential for the motor losses since the copper losses dominate it. Due to the nonlinearities in this machine with the resultant distributed influence of geometrical variables on performance, all variables will be considered in DE process for best output.

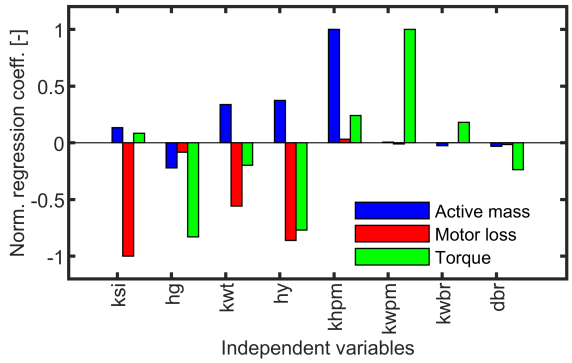

Fig. 3. Normalized nonlinear regression coefficients showing the influence of independent variables at peak loading and expected high operating temperature on the active mass, motor loss, and torque.

Table I
INDEPENDENT VARIABLES AND THEIR RANGES FOR OPTIMIZATION OF THE SPOKE IPM.

Variable	Description	Min	Max
ksi	split ratio	0.60	0.75
kwt	stator teeth width ratio	0.45	0.75
khpm	PM length ratio	0.55	0.95
kwpm	PM width ratio	0.20	0.60
kwbr	rotor bridge width ratio	0.35	0.65
hg	airgap [mm]	0.70	2.50
hy	stator yoke thickness [mm]	7.00	15.00
dbr	rotor bridge length [mm]	0.20	0.35

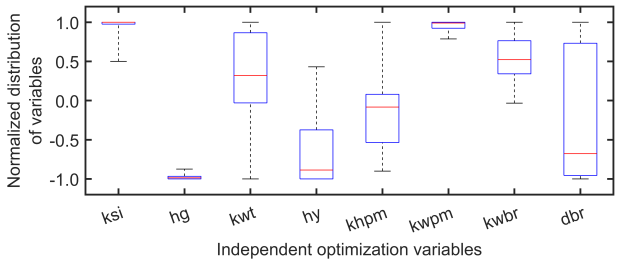

Fig. 4. The distribution of variables for optimal Pareto front designs in an 18-slot, 16-pole spoke-type IPM configuration indicates that a minimal air gap is preferable, along with thicker PMs oriented in the direction of magnetization in line with expectation.

B. Differential Evolution (DE)

Metrics related to motor active mass and losses are crucial for optimizing cost and efficiency in the large-scale production of electric motors. The parametric model of the spoke IPM shown in Fig. 2 considering an outermost diameter of 160mm was, therefore, analyzed for an objective torque, T_e, of 110Nm at a base speed of 6,000rpm typical for specialized applications in electric traction [16], [36], [39].

In addition to meeting the torque requirement, the motor topology under investigation is *optimized* for two concurrent objectives which are to *minimize* the active mass, F_1, and motor loss, F_2:

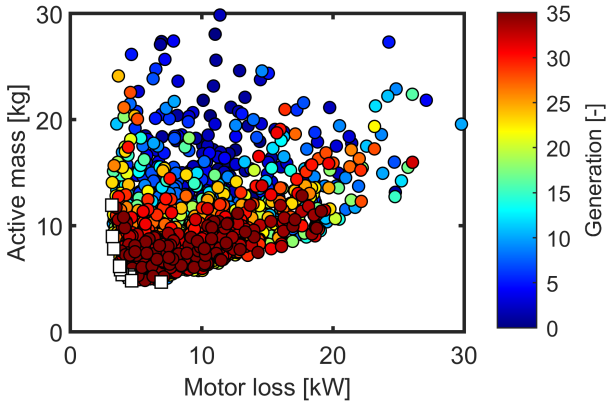

Fig. 5. Optimization results obtained using MODE for the spoke IPM topology for the objectives of active mass and motor loss. The Pareto designs are shown in white, coming mostly in the last generations with a compromise between the two objectives in line with expectations.

$$\begin{aligned} F_1 &= m_{Fe} + m_{Cu} + m_{PM}, \\ F_2 &= P_{loss} = P_{Fe} + P_{Cu} + P_{PM}, \end{aligned} \tag{3}$$

where m_{Fe} is the mass of laminated steel, m_{Cu} the mass of copper, and m_{pm} the mass of the PMs. The objective function for motor loss, P_{loss}, was calculated as the sum of the variable and constant losses of the motor, where P_{Fe} represents the core loss (constant losses), P_{PM} represents the eddy losses in the PMs, and P_{Cu} represents the copper loss (variable losses). These losses were computed for the anticipated high operating temperature of 120^{o}C. To account for potential PM demagnetization, a constraint was imposed to ensure that the minimum flux density in the PMs of output designs remains above 40% at the specified high operating temperature.

The DE algorithm follows a well-researched and extensively used format first proposed by Storn and Price in 1995. The algorithm progresses through generations, where each generation undergoes specific steps: initialization, mutation, crossover, and selection [5]. Considering the 8 independent geometrical variables of the spoke IPM topology, 70 design candidates are considered in each generation of the DE optimization. A two-pass procedure within the DE ensures that each design meets the required rated torque of 110Nm at the defined base speed. Initially, torque was calculated using FEA, and then the stack length, ℓ_{stk}, was adjusted to achieve the specified rated torque before evaluating set optimization objectives and other performance criteria.

To enhance the optimization's computational efficiency, a hybrid stopping condition was applied, which halts the process either after reaching the maximum number of generations or when minimal improvements ($<$1%) were detected in three key points of the Pareto front over successive generations. To further validate that the optimal ranges had been correctly set for the independent variables, box plots displaying their distribution for the Pareto designs were examined, as shown in Fig. 4. As expected, the optimal designs favored a minimal air gap and thicker PM widths in the direction of magnetization.

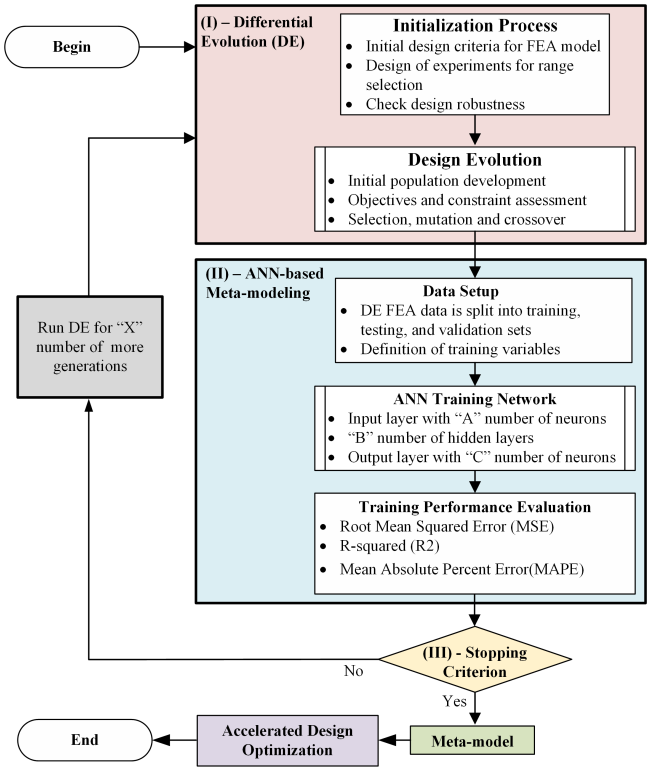

Fig. 6. A flowchart illustrating the stages of the proposed ANN-based meta-modeling approach, employing differential evolution as the input stage, where A, B, C, and X are integer parameters. A stopping criterion based on set test metrics checks training satisfaction, and afterward, a resultant meta-model can be obtained.

IV. ANN-BASED META-MODELING

Given that the spoke IPM is a highly saturated machine with inherent nonlinear relationships between geometry and performance, the development of a meta-model trained on performance results from FEA of designs generated by DE optimization could provide insights into the feasibility of performance estimation through meta-modeling. This could offer the potential benefits of reduced computational effort and increased flexibility.

Using TensorFlow [40], ANN meta-models were developed and trained using the results of DE to predict the ratio, T_e/ℓ_{stk}, and P_{Fe} for spoke IPM machine designs. The implemented mode of the ANN comprises one input layer, three hidden layers with 128, 64, and 32 neurons, respectively, and one output layer with 1 neuron. The proposed approach is directly integrated into the design process, as shown in Fig. 6, with the performance of the meta-model being monitored using error metrics with every successive DE generation whose data was fed as input. A stopping criterion was also proposed to assess the adequacy of the meta-model; this could include user-set error values, time elapsed, number of DE generations, or a combination in between.

Two ANN models were trained on a dataset of 2,500 candidate designs generated through 2D FEA-based DE optimization (Fig. 5). The ANN model for predicting the ratio

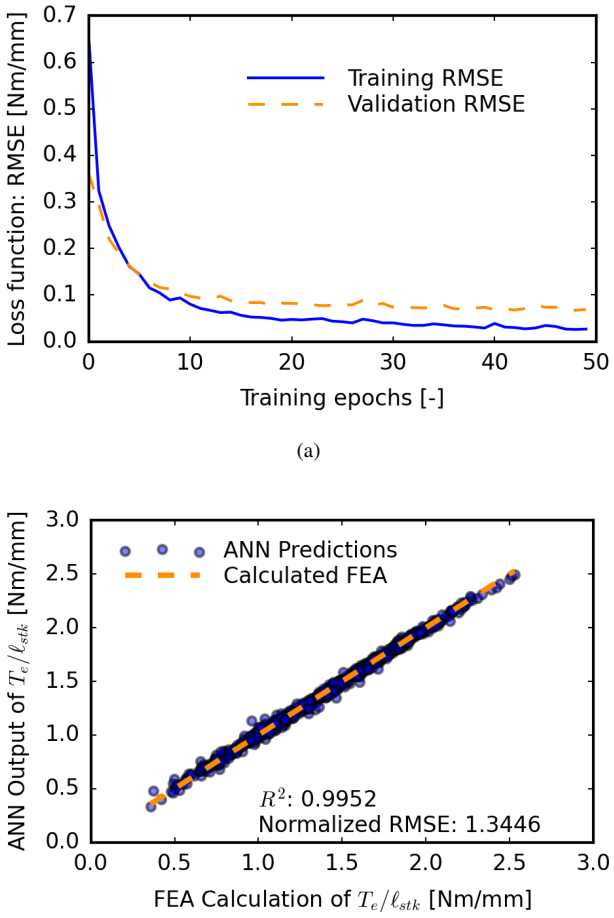

Fig. 7. The output trends for the ANN-based meta-modeling for the ratio T_e/ℓ_{stk} show: (a) The progression of the RMSE for the training and validation sets over all 50 epochs. A rapid decline during the first 10 epochs and stabilization afterward indicate effective learning. (b) the regression curve between ANN predicted and FEA calculations with the resulting R^2 and normalized RMSE indicating high accuracy.

T_e/ℓ_{stk} was trained using 8 geometric input parameters described in Fig. 2, while the model for P_{Fe} included these same parameters along with the stack length, totaling 9 input variables. The copper losses, P_{Cu}, can be computed using mathematical formulations since the fixed current density and geometry of the coils are known. From the candidate designs, a random selection of 50% was employed for training, 30% for validation, and the remaining 20% for testing the ANN meta-model.

V. RESULTS AND DISCUSSION

The ANN's generalization was assessed by comparing RMSE values for training and validation datasets over 50 epochs as shown in Fig. 7a. The close alignment of the curves indicates effective generalization without overfitting. The performance of the ANN meta-models was evaluated based on typical metrics of R-squared (R^2), normalized root

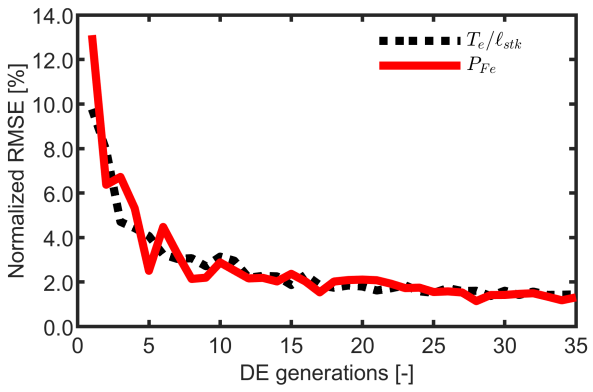

Fig. 8. The progression of normalized RMSE with increasing DE generational data shows a decrease in the error with more training across the generations.

mean square error (NRMSE), and mean absolute percentage error (MAPE) metrics.

The torque-to-stack-length ratio model, T_e/ℓ_{stk}, achieved an R^2 of 0.9952, reflecting a strong alignment between predictions and FEA outputs, as shown in Fig. 7b. The NRMSE of 1.34% and MAPE of 1.83% illustrated that the model was highly accurate in estimating the torque-to-stack-length ratio across varying designs. For the core loss model, P_{Fe}, an R^2 value of 0.9906 demonstrates a high correlation between the ANN predictions and the FEA results, while the low NRMSE of 1.31% confirms the precision of the predictions. The mean absolute percentage error (MAPE) of 3.41% further supports this stance, showing that the ANN predictions deviate minimally from the calculated values.

The error reduction during training, as seen in Fig. 8, highlights the robustness of the ANN. Both models exhibit a rapid decline in NRMSE within the first 10 generations of the differential evolution (DE) optimization process, signifying their ability to learn the nonlinear patterns in the dataset. This suggests the meta-model can replace the FEA in the design optimization after, for example, the 20th generation with NRMSE of about 2%, potentially reducing computational effort by a third.

The low error values and accurate predictions of the ANN models demonstrate their ability to capture the nonlinear relationships in T_e/ℓ_{stk} and P_{Fe}. This highlights their generalization capabilities and suitability as meta-models for electromagnetic design tasks. These results confirm the viability as a computationally efficient meta-model, minimizing computational efforts while maintaining high accuracy.

VI. Conclusion

The feasibility of employing ANN meta-models, trained with minimal data from DE, to predict performance metrics for highly saturated, nonlinear spoke-type IPM designs was successfully demonstrated, providing an efficient alternative to traditional FEA. The ANN meta-models for torque-to-stack-length ratio (T_e/ℓ_{stk}) and core loss (P_{Fe}) achieved high accuracy, with R^2 values of 0.9952 and 0.9906, and NRMSEs of 1.34% and 1.31%. Their NRMSE dropped to about 2% by the 20th DE generation, at which point the FEA could be replaced, saving up to a third of the computational time.

The low error values and robust predictions of the ANN models demonstrate their potential as computationally efficient surrogates for design optimization. By utilizing reduced DE generation data, the meta-model can be trained to emulate and used directly in optimization studies, thereby accelerating the motor design optimization process exponentially and potentially allowing for large-scale system-level optimization, including, for example, drive cycle analysis.

Acknowledgment

The support of ANSYS Inc., University of Kentucky, the L. Stanley Pigman Chair in Power Endowment, and the National Science Foundation (NSF) Graduate Research Fellowship under Grant No. 223906 is gratefully acknowledged. Any opinions, findings, and conclusions or recommendations expressed in this material are those of the authors and do not necessarily reflect the views of the sponsoring organizations.

References

[1] B. Fahimi, L. H. Lewis, J. M. Miller, S. D. Pekarek, I. Boldea, B. Ozpineci, K. Hameyer, S. Schulz, A. Ghaderi, M. Popescu, B. Lehman, and D. D. Patel, "Automotive electric propulsion systems: A technology outlook," *IEEE Transactions on Transportation Electrification*, pp. 1–1, 2023.

[2] M. Helbing, S. Uebel, C. Matthes, and B. Bäker, "Comparative case study of a metamodel-based electric vehicle powertrain design," *IEEE Access*, vol. 9, pp. 160 823–160 835, 2021.

[3] O. A. Badewa and D. M. Ionel, "Comparative analysis of motors with inner and outer reluctance rotors and PM stators," in *2024 IEEE Transportation Electrification Conference and Expo (ITEC)*, 2024, pp. 1–6.

[4] V. Parekh, D. Flore, and S. Schöps, "Deep learning-based meta-modeling for multi-objective technology optimization of electrical machines," *IEEE Access*, vol. 11, pp. 93 420–93 430, 2023.

[5] M. Rosu, P. Zhou, D. Lin, D. M. Ionel, M. Popescu, F. Blaabjerg, V. Rallabandi, and D. Staton, *Multiphysics simulation by design for electrical machines, power electronics and drives*. John Wiley & Sons, 2017.

[6] H. Barua, L. Lin, V. Rallabandi, J. Wilkins, P. Kumar, and B. Ozpineci, "Mechanical and vibration analysis of a high-speed outer rotor electric motor," *IEEE Access*, vol. 12, pp. 137 881–137 892, 2024.

[7] M. Popescu, J. Goss, D. A. Staton, D. Hawkins, Y. C. Chong, and A. Boglietti, "Electrical vehicles—practical solutions for power traction motor systems," *IEEE Transactions on Industry Applications*, vol. 54, no. 3, pp. 2751–2762, 2018.

[8] M. Popescu, L. Di Leonardo, G. Fabri, G. Volpe, N. Riviere, and M. Villani, "Design of induction motors with flat wires and copper rotor for E-Vehicles traction system," *IEEE Transactions on Industry Applications*, vol. 59, no. 3, pp. 3889–3900, 2023.

[9] N. Bianchi, S. Bolognani, E. Carraro, M. Castiello, and E. Fornasiero, "Electric vehicle traction based on synchronous reluctance motors," *IEEE Transactions on Industry Applications*, vol. 52, no. 6, pp. 4762–4769, 2016.

[10] A. Credo, M. Villani, G. Fabri, and M. Popescu, "Adoption of the synchronous reluctance motor in electric vehicles: A focus on the flux weakening capability," *IEEE Transactions on Transportation Electrification*, vol. 9, no. 1, pp. 805–818, 2023.

[11] Z. Yang, F. Shang, I. P. Brown, and M. Krishnamurthy, "Comparative study of interior permanent magnet, induction, and switched reluctance motor drives for EV and HEV applications," *IEEE Transactions on Transportation Electrification*, vol. 1, no. 3, pp. 245–254, 2015.

[12] J. Godbehere, M. Popescu, and M. Michon, "Optimization of an IPM traction motor considering the electric drive unit system requirements," in *2021 IEEE Energy Conversion Congress and Exposition (ECCE)*, 2021, pp. 3667–3674.

[13] P. Asef, R. Bargallo, A. Lapthorn, D. Tavernini, L. Shao, and A. Sorniotti, "Assessment of the energy consumption and drivability performance of an IPMSM-driven electric vehicle using different buried magnet arrangements," *Energies*, vol. 14, no. 5, 2021. [Online]. Available: https://www.mdpi.com/1996-1073/14/5/1418

[14] A. Allca-Pekarovic, P. J. Kollmeyer, A. Forsyth, and A. Emadi, "Experimental characterization and modeling of a YASA P400 axial flux PM traction machine for performance analysis of a chevy bolt EV," *IEEE Transactions on Industry Applications*, vol. 60, no. 2, pp. 3108–3119, 2024.

[15] D. Winterborne, N. Stannard, L. Sjöberg, and G. Atkinson, "An air-cooled YASA motor for in-wheel electric vehicle applications," *IEEE Transactions on Industry Applications*, vol. 56, no. 6, pp. 6448–6455, 2020.

[16] A. Fatemi, D. M. Ionel, M. Popescu, Y. C. Chong, and N. A. O. Demerdash, "Design optimization of a high torque density spoke-type PM motor for a formula E race drive cycle," *IEEE Transactions on Industry Applications*, vol. 54, no. 5, pp. 4343–4354, 2018.

[17] A. Fatemi, "Design optimization of permanent magnet machines over a target operating cycle using computationally efficient techniques," Ph.D. dissertation, Marquette University, 2016.

[18] C. S. Goli, M. G. Kesgin, P. Han, D. M. Ionel, S. Essakiappan, J. Gafford, and M. D. Manjrekar, "Analysis and design of an electric machine employing a special stator with phase winding modules and PMs and a reluctance rotor," *IEEE Access*, vol. 12, pp. 9621–9631, 2024.

[19] O. A. Badewa and D. M. Ionel, "Analysis and design of synchronous machines with reluctance rotor and PM stator combined excitation," in *2024 IEEE Energy Conversion Congress and Exposition (ECCE)*, 2024, pp. 1–6.

[20] O. A. Badewa, A. Mohammadi, D. D. Lewis, S. Essakiappan, M. Manjrekar, and D. M. Ionel, "Electromagnetic design characterization of synchronous machines with flux switching effect employing reluctance rotors and stators with PMs and AC concentrated coils," *IEEE Transactions on Industry Applications*, pp. 1–14, 2025.

[21] M. Gobbi, A. Sattar, R. Palazzetti, and G. Mastinu, "Traction motors for electric vehicles: Maximization of mechanical efficiency–a review," *Applied Energy*, vol. 357, p. 122496, 2024.

[22] O. A. Badewa, A. Mohammadi, D. D. Lewis, and D. M. Ionel, "Optimal design and comparison of synchronous machines with inner and outer reluctance rotors and PM or DC stator combined excitation," in *2024 IEEE Energy Conversion Congress and Exposition (ECCE)*, 2024, pp. 1–5.

[23] M. Omar, M. Bakr, and A. Emadi, "Switched reluctance motor design optimization: A framework for effective machine learning algorithm selection and evaluation," in *2024 IEEE Transportation Electrification Conference and Expo (ITEC)*, 2024, pp. 1–6.

[24] D. Barri, F. Soresini, M. Gobbi, A. d. Gerlando, and G. Mastinu, "Optimal design of traction electric motors by a new adaptive pareto algorithm," *IEEE Transactions on Vehicular Technology*, pp. 1–17, 2025.

[25] B. F. Azevedo, A. M. A. Rocha, and A. I. Pereira, "Hybrid approaches to optimization and machine learning methods: a systematic literature review," *Machine Learning*, pp. 1–43, 2024.

[26] O. Borsboom, M. Salazar, and T. Hofman, "Design optimization of electric vehicle drivetrains using surrogate modeling frameworks," *Authorea Preprints*, 2025.

[27] M. Cheng, X. Zhao, M. Dhimish, W. Qiu, and S. Niu, "A review of data-driven surrogate models for design optimization of electric motors," *IEEE Transactions on Transportation Electrification*, pp. 1–1, 2024.

[28] A.-C. Pop, Z. Cai, and J. J. C. Gyselinck, "Machine-learning aided multiobjective optimization of electric machines— geometric-feasibility and enhanced regression models," *IEEE Journal of Emerging and Selected Topics in Industrial Electronics*, vol. 4, no. 3, pp. 844–854, 2023.

[29] H. Sasaki, Y. Hidaka, and H. Igarashi, "Prediction of IPM machine torque characteristics using deep learning based on magnetic field distribution," *IEEE Access*, vol. 10, pp. 60 814–60 822, 2022.

[30] H. Wu, S. Niu, Y. Zhang, X. Zhao, and W. Fu, "Fast magnetic field approximation method for simulation of coaxial magnetic gears using AI," *IEEE Journal of Emerging and Selected Topics in Industrial Electronics*, vol. 4, no. 1, pp. 400–408, 2023.

[31] L. Liu, Z. Li, H. Kang, Y. Xiao, L. Sun, H. Zhao, Z. Zhu, and Y. Ma, "Review of surrogate model assisted multi-objective design optimization of electrical machines: New opportunities and challenges," *Renewable and Sustainable Energy Reviews*, vol. 215, p. 115609, 2025. [Online]. Available: https://www.sciencedirect.com/science/article/pii/S1364032125002825

[32] N. Taran, D. M. Ionel, and D. G. Dorrell, "Two-level surrogate-assisted differential evolution multi-objective optimization of electric machines using 3-D FEA," *IEEE Transactions on Magnetics*, vol. 54, no. 11, pp. 1–5, 2018.

[33] C. He, Y. Zhang, D. Gong, and X. Ji, "A review of surrogate-assisted evolutionary algorithms for expensive optimization problems," *Expert Systems with Applications*, vol. 217, p. 119495, 2023.

[34] G. Volpe, J. Goss, I. Foley, F. Marignetti, M. Popescu, and D. A. Staton, "High-performance electric motor for motor sport application," in *2017 IEEE Vehicle Power and Propulsion Conference (VPPC)*, 2017, pp. 1–5.

[35] G.-H. Kang, J. Hur, H.-G. Sung, and J.-P. Hong, "Optimal design of spoke type BLDC motor considering irreversible demagnetization of permanent magnet," in *Sixth International Conference on Electrical Machines and Systems, 2003. ICEMS 2003.*, vol. 1, 2003, pp. 234–237 vol.1.

[36] M. Popescu, I. Foley, D. A. Staton, and J. E. Goss, "Multi-physics analysis of a high torque density motor for electric racing cars," in *2015 IEEE Energy Conversion Congress and Exposition (ECCE)*, 2015, pp. 6537–6544.

[37] *Ansys® Electronics, version 24.1, 2024, ANSYS Inc.*

[38] P. Asef and A. Lapthorn, "Overview of sensitivity analysis methods capabilities for traction AC machines in electrified vehicles," *IEEE Access*, vol. 9, pp. 23 454–23 471, 2021.

[39] P. Asef and C. Vagg, "A physics-informed bayesian optimization method for rapid development of electrical machines," *Scientific Reports*, vol. 14, no. 1, p. 4526, 2024.

[40] M. Abadi *et al.*, "TensorFlow: Large-scale machine learning on heterogeneous systems," 2015, software available from tensorflow.org. [Online]. Available: https://www.tensorflow.org/